

Weather in mesospheric ice layers

U. Berger¹ and F.-J. Lübken¹

Received 18 October 2005; revised 30 November 2005; accepted 17 January 2006; published 28 February 2006.

[1] Layers in the summer mesosphere are studied using an ice model which applies background conditions from a new model called LIMA (Leibniz Institute Middle Atmosphere Model). LIMA covers the height range 0–150 km with high resolution. At low altitudes LIMA assimilates ECMWF ERA 40 data which introduces variability in the upper atmosphere. LIMA adequately represents the conditions in the mesosphere/lower thermosphere. Ice formation is interactively coupled to background water vapour which leads to ‘freeze drying’. Model ice layers vary in time and space and occasionally appear at mid latitudes. The geographical distribution of ice clouds generally agrees with observations. For example, the mean noctilucent cloud height at 69°N is 83.8 km (observations: 83.3 km). The occurrence rates of (polar) mesosphere summer echoes from the model also agree with measurements. At high latitudes ice layers sometimes disappear (‘ice holes’). From time to time wind fluctuations redistribute water vapor but in general freeze drying overwhelms. **Citation:** Berger, U., and F.-J. Lübken (2006), Weather in mesospheric ice layers, *Geophys. Res. Lett.*, 33, L04806, doi:10.1029/2005GL024841.

1. Introduction

[2] Ice particles exist close to the summer mesopause at mid and polar latitudes and are known as ‘noctilucent clouds’, NLC, or ‘polar mesospheric clouds’, PMC, depending on the observation geometry, i. e., from the ground by naked eye and lidars, or from satellites. They can also lead to strong radar echoes known as ‘(polar) mesosphere summer echoes’, (P)MSE. For more details, see *Fiedler et al.* [2003], *Rapp and Lübken* [2004], and *Bailey et al.* [2005, and references therein]. The characteristic properties of these layers such as mean altitude, occurrence frequency, brightness, and geographical distribution are frequently used to infer information about the background atmosphere, for example long term variations or hemispherical differences [see, e.g., *Chu et al.*, 2004]. This approach is tempting since ice particle formation is very sensitive to the background, most important to temperature and water vapor concentration. Model studies normally use quasi-stationary background conditions which can lead to spurious results. For example, according to the mean thermal structure one would not expect to observe NLC or MSE at a mid latitude station like Kühlungsborn (54°N). However, these ice-related phenomena are frequently detected here [*Zecha et al.*, 2003] which is presumably due to short term deviations of the atmosphere from the mean state and/or because ice clouds drift from polar to mid latitudes.

[3] The effect of short term gravity wave variations on NLC has been studied previously but assuming stationary background conditions [*Rapp et al.*, 2002]. In the model study presented in this paper the atmosphere varies with time, latitude, and longitude, similar to a previous version published by *von Zahn and Berger* [2003]. Major improvements have been made recently by introducing realistic day-to-day variability generated through coupling with the troposphere and stratosphere. At the same time the model grid structure and size was significantly improved to cover these small scales. In this paper we study the influence of atmospheric variations on ice layers, in particular on their geographical distribution. The day-to-day variation of ice layer properties led us to introduce the term ‘weather’ for this phenomenon.

2. Ice Layers Within the LIMA Atmosphere Model

[4] Based on our previous atmospheric model called COMMA/IAP (Cologne Model of the Middle Atmosphere/Institute of Atmospheric Physics) we have developed a new 3D GCM model called LIMA (Leibniz Institute Middle Atmosphere Model) which exhibits major improvements regarding dynamical structures. We will not describe LIMA in this paper but instead refer to U. Berger and F.-J. Lübken (LIMA: A new model of the upper atmosphere, manuscript in preparation, 2006). for more details. Here we only briefly discuss those features which are crucial for ice particle formation. LIMA covers the height range 0–150 km on a global scale and contains all relevant physical and chemical processes, such as dynamics, radiation, chemistry, and transport. The model applies a time step of 150 seconds and a triangle grid structure with 41,248 grid points. The horizontal and vertical resolution is approximately 110 km and 1 km, respectively. In the height range 0–35 km LIMA assimilates the ERA-40 reanalysis data of ECMWF every 6 hours through a ‘nudging technique’. This introduces spatial and temporal variability not only in this height range but also in the upper atmosphere. In Figure 1 we show a time series of temperatures at 69°N, 16°E, for 110 days using lower atmosphere conditions from May 20 until September 10, 2001. LIMA temperatures nicely agree with the experimental climatology presented by *Lübken* [1999]. For example, during July the mesopause is located at ~88 km with temperatures less than 135 K. At 82 km the temperature is close to 150 K. Furthermore, typical variations in the upper atmosphere are on the order of ±5 K, again in agreement with observations [see *Lübken*, 1999, Figure 7]. Similar to Figure 1, variability is present in all relevant atmospheric parameters, in particular in horizontal and vertical winds, pressure, densities, water vapor etc. LIMA correctly describes the mean background conditions at mid and high latitudes. Details of this model are not

¹Leibniz Institute of Atmospheric Physics, Kühlungsborn, Germany.

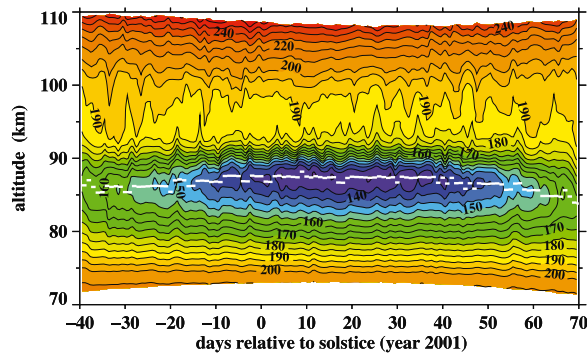


Figure 1. Temperatures over Andøya (69°N, 16°E) from LIMA using lower atmosphere conditions for May 20 until September 10, 2001. The white broken line indicates the mesopause altitude.

important in this context since it is used ‘only’ as the background in which the ice layer develops.

[5] An ice model is super-imposed on LIMA similar to a former version described by *Berger and von Zahn* [2002] (hereafter referred to as BvZ02). The ice model runs with a time step of 45 seconds and covers the latitude band from 37.5° to 90° (in both hemispheres) and heights from 78 to 94 km. It is updated once per day (at 00:00 UT) with LIMA background winds, temperatures, and total air mass densities. In between these updates the background fields are linearly interpolated. After initialization at May 31 a dust cloud is transported with the background wind and forms ice particles if the conditions are appropriate. The formation, transport, and sublimation of ice particles is interactively coupled to water vapor at each time step (45 seconds) which thereby can lead to a depletion of H₂O known as ‘freeze drying’. These changes in water vapor are not yet fed back to the dynamical/chemical/radiative part of LIMA. This implies that the redistribution of water vapor does not effect other minor constituents (e.g., OH) nor the circulation and temperatures within LIMA. The microphysics of ice particle formation in our model is similar to BvZ02 but we have adapted some new results from the comprehensive

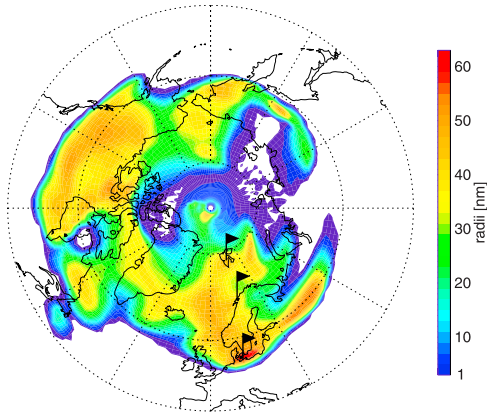


Figure 2. Snapshot of the maximum modal ice radius in a vertical column on July 2001, 00:00 UT. Three stations are marked by a flag: Kühlungsborn (54°N), ALOMAR (69°N), and Spitsbergen (78°N).

review by *Rapp and Thomas* [2005]. For example, we have used the expression for the saturation pressure of water vapor over ice from *Marti and Mauersberger* [1993]. The ice model runs with a spatial resolution of 100 m in the vertical, and 3° and 1° in the zonal and meridional plane, respectively.

3. Layer Characteristics

[6] In Figure 2 a snapshot of the geographical distribution of the maximum modal ice radius is shown for conditions in the lower atmosphere from July 23, 2001, 00:00 UT. This plot shows striking similarities with satellite observations of ice clouds [*Merkel et al.*, 2003]. There are various regions where ice particles with radii larger than 40–50 nm occur which are typical radii deduced from multi-color lidar observations of NLC [*von Cossart et al.*, 1999]. The ice cloud in Figure 2 shows significant geographical variability and at this particular time reaches Kühlungsborn. The cloud develops in time and space and occasionally extends to much lower latitudes than expected from mean mesosphere temperatures. Indeed, NLC have been observed as far south as Logan (41.7°N) where mean mesopause temperatures are much too large for ice particles [*Wickwar et al.*, 2002]. In Figure 2 there are also major patches where the maximum ice radius is smaller than 10–20 nm, i.e., too small to be detectable by lidars but still large enough to create PMSE. This explains why the occurrence rate of PMSE is generally larger than NLC [*Rapp and Lübken*, 2004].

[7] For comparison with our lidar measurements of NLC at ALOMAR we have extracted the ice cloud characteristics at 69°N and calculated the modal ice radius and backscatter coefficients (β) at a wavelength of $\lambda = 532$ nm for a 20 day period in mid summer (see Figure 3). Indeed, the mean characteristics of the modeled NLC are similar to observations [*Fiedler et al.*, 2003]. We have used a lower limit of $\beta = 4 \cdot 10^{-10}/(\text{sr} \cdot \text{m})$ in Figure 3 to reflect typical sensitivities of modern lidar systems. The NLC is intermittent and its strength varies with time and height. Backscatter

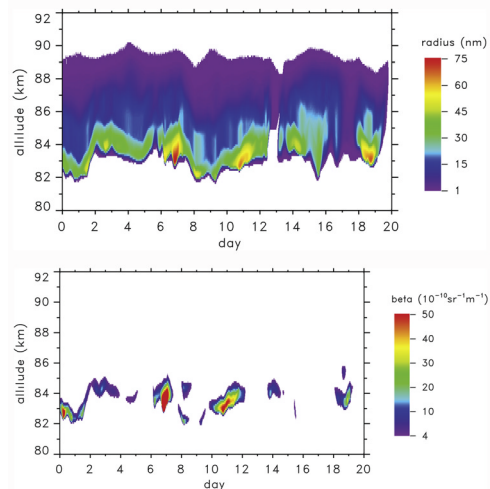


Figure 3. Three weeks of ice cloud model results during mid summer (10–31 July) at 69°N, 16°E. (top) Particle radii. (bottom) Backscatter coefficient for a lidar operating at 532 nm.

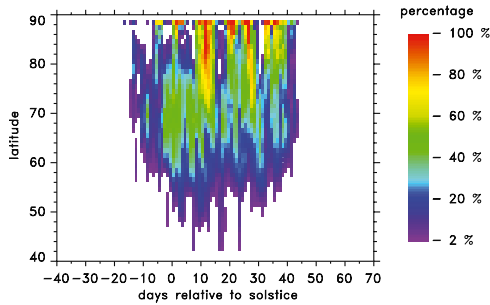


Figure 4. LIMA/ice model result of the seasonal and latitudinal distribution of NLC occurrence rates in the northern hemisphere. Daily occurrence rates were determined along latitudinal circles applying a threshold of $\beta = 4 \cdot 10^{-10}/(\text{sr} \cdot \text{m})$ (β = backscatter coefficient at a wavelength of $\lambda = 532 \text{ nm}$).

coefficients are typically some $10^{-9}/(\text{sr} \cdot \text{m})$. Considering an entire NLC season we find from our model a mean centroid altitude of $z_c = 83.8 \text{ km}$, similar to observations ($z_c = 83.3 \text{ km}$ [see *Fiedler et al.*, 2003]). In agreement with former models and observations small ice particles are present up to $\sim 90 \text{ km}$. Above $\sim 85 \text{ km}$ they are too small to be seen by lidar, but they can be detected by in-situ methods and they can still create strong radar echoes [*Havnes et al.*, 1996]. The occurrence frequency of NLC at ALOMAR calculated from our LIMA/ice model for the period June 1 until August 31 is 26%, again similar to observations [see *Fiedler et al.*, 2003, Figure 3].

[8] In Figure 4 we show the LIMA/ice model result of the seasonal and altitudinal distribution of NLC occurrence rate in the northern hemisphere. We define occurrence rate as the daily number of bins (relative to the total number) on a latitudinal circle where the backscatter coefficient exceeds a threshold of $\beta = 4 \cdot 10^{-10}/(\text{sr} \cdot \text{m})$ (similar to Figure 3). We also take Figure 4 as a representation of polar mesospheric clouds (PMC) (i.e., satellite borne observations of ice clouds), realizing that differences will most likely occur due to instrumental specifications such as wavelength, scattering angle, sensitivity etc. However, the general picture will most likely be unchanged. The daily occurrence rate in Figure 4 generally increases with latitude but shows significant seasonal and temporal variability in agreement with PMC observations [*Bailey et al.*, 2005]. Ice particles can disappear almost entirely at very high latitudes from time to time (see, for example, around day 32 at $\sim 84^\circ\text{N}$). These ‘ice holes’ have been observed from satellites and also in PMSE at Spitsbergen [*Bailey et al.*, 2005; *Lübken et al.*, 2004]. We see from the temporal development of the background field and the ice particle distribution that ice holes are created by extremely dry and ice free air which drifts from higher altitudes and/or from other geographical locations.

[9] We have determined the occurrence rate of (polar) mesosphere summer echoes by calculating the proxy $P = r_A^2 \cdot Z_A \cdot N_A$, where r_A is the particle radius, Z_A their charge, and N_A their number number density [*Rapp et al.*, 2003]. In Figure 5 we show the seasonal variation of PMSE occurrence rates for three stations, namely Kühlungsborn (54°N), ALOMAR (69°N), and Spitsbergen (78°N). The occurrence

rate in Figure 5 is defined as the daily number of bins (relative to the total number) where $P > 100 \text{ nm}^2 \cdot \text{e}^-/\text{cm}^3$ on a latitudinal circle at any altitude. From our model we find typical mid-summer occurrence rates of 18%, 76%, and 93% at 54°N , 69°N , and 78°N , respectively. The proxy threshold from above is somewhat arbitrary since PMSE detection critically depends on radar specifications. This makes a comparison with observations difficult and requires a ‘calibration’ of the proxy. Furthermore, neutral air turbulence is a key element in producing PMSE and is not considered in the proxy. Very little is known about the seasonal and latitudinal variation of turbulence. Taking these limitations into account the agreement of our model results with observations is remarkable. For example, observed mid summer occurrence rates of PMSE are typically 10%, 80–90%, and 100% at 54°N , 69°N , and 78°N , respectively, consistent with the numbers stated above [*Zecha et al.*, 2003; *Bremer et al.*, 2003; *Lübken et al.*, 2004]. The PMSE season at polar latitudes in Figure 5 starts close to June 1 (ends around 15 August) which is again close to observations but somewhat late (early) by a few days.

4. Discussion

[10] The ice cloud fluctuations presented above are partly generated through the variable background atmosphere. Other atmospheric parameters, in particular water vapor, are modified through ice particle formation which further enhances their variability. The update rate of the background atmosphere is currently once per day. This limitation is mainly given by computer resources and will be improved in the future. We will then be able to include processes on even smaller temporal and spatial scales, for example, gravity waves. Gravity waves can enhance or destroy ice particles, depending on the wave period [*Rapp et al.*, 2002]. In this paper we assume that gravity waves and tides have no major effect on the general morphology of ice layers, in particular not on their geographical distribution.

[11] We have used lower atmosphere conditions from the summer of 2001 in our studies. Whether or not our simulation of ice layers in the mesosphere shows detailed similarities with observations in that particular year is subject of future studies.

[12] A redistribution of water vapor through ice particle generation, transport, diffusion, photolysis, and sublimation

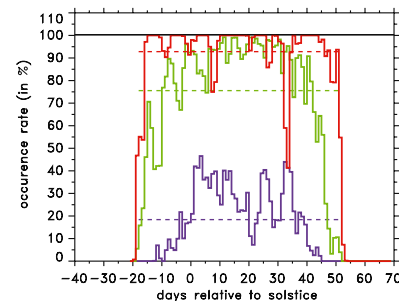


Figure 5. Model result of the seasonal variation of PMSE occurrence rates at three latitudes, namely, 54°N (blue), 69°N (green), and 78°N (red). The dashed lines indicate mean values in the period June 1 until August 10.

has been observed in the model of BvZ02 which, however, did not consider small and medium scale atmospheric variability. Our LIMA/ice model shows that these fluctuations can indeed temporarily redistribute water vapor in the upper mesosphere and drive the concentration back to the undisturbed state. In general, however, freeze drying overwhelms and significantly reduces the total water vapor content in the upper mesosphere. The redistribution of water vapor leads to a significant drying in the entire polar region and to an accumulation of water vapor at mid latitudes where ice particles preferably sublimate. This can locally and sporadically increase the water vapor concentration to 10–20 ppm, i.e., an order of magnitude above the background. These moist regions support the formation of ice particles at lower latitudes.

[13] We have shown that the geographical distribution of mean ice layer characteristics derived from our model are consistent with lidar, satellite, and radar observations. For the first time we have been able to reproduce the occasional appearance of NLC and PMSE at mid latitudes where mean temperatures are generally too large for ice particles. The LIMA/ice model offers the unique chance to study the effect of background atmosphere changes on NLC, PMC, and PMSE, in particular regarding their geophysical distribution and long term variation caused by solar cycle and anthropogenic influences. In the future we plan to study in detail the cause of regional and interhemispheric differences, for example, the SH/NH difference in PMC and PMSE occurrence, the longitudinal variation of PMSE at high latitudes, and the feedback effect of water vapor redistribution on the thermal and dynamical structure of the atmosphere.

[14] **Acknowledgments.** We acknowledge the assistance of Florian Herbot and Boris Strelnikov in producing the figures. We thank Markus Rapp for valuable comments. This project was supported by the SOLEIL project (grant LU 1174) of the German Research Foundation (DFG).

References

- Bailey, S. M., A. W. Merkel, G. E. Thomas, and J. N. Carstens (2005), Observations of polar mesospheric clouds by the Student Nitric Oxide Explorer, *J. Geophys. Res.*, *110*, D13203, doi:10.1029/2004JD005422.
- Berger, U., and U. von Zahn (2002), Icy particles in the summer mesopause region: Three-dimensional modeling of their environment and two-dimensional modeling of their transport, *J. Geophys. Res.*, *107*(A11), 1366, doi:10.1029/2001JA000316.
- Bremer, J., P. Hoffmann, R. Latteck, and W. Singer (2003), Seasonal and long-term variations of PMSE from VHF radar observations at Andenes, Norway, *J. Geophys. Res.*, *108*(D8), 8438, doi:10.1029/2002JD002369.
- Chu, X., G. J. Nott, P. J. Espy, C. S. Gardner, J. C. Diettrich, M. A. Clilverd, and M. J. Jarvis (2004), Lidar observations of polar mesospheric clouds at Rothera, Antarctica, 67.5°S, 68.0°W, *Geophys. Res. Lett.*, *31*, L02114, doi:10.1029/2003GL018638.
- Fiedler, J., G. Baumgarten, and G. von Cossart (2003), Noctilucent clouds above ALOMAR between 1997 and 2001: Occurrence and properties, *J. Geophys. Res.*, *108*(D8), 8453, doi:10.1029/2002JD002419.
- Havnes, O., J. Trøim, T. Blix, W. Mortensen, L. I. Næsheim, E. Thrane, and T. Tønnesen (1996), First detection of charged dust particles in the Earth's mesosphere, *J. Geophys. Res.*, *101*, 10,839–10,847.
- Lübken, F.-J. (1999), Thermal structure of the Arctic summer mesosphere, *J. Geophys. Res.*, *104*, 9135–9149.
- Lübken, F.-J., M. Zecha, J. Höffner, and J. Röttger (2004), Temperatures, polar mesosphere summer echoes, and noctilucent clouds over Spitsbergen (78°N), *J. Geophys. Res.*, *109*, D11203, doi:10.1029/2003JD004247.
- Marti, J., and K. Mauersberger (1993), A survey and new measurements of ice vapor pressure at temperatures between 170 and 250 K, *Geophys. Res. Lett.*, *20*, 363–366.
- Merkel, A. W., G. E. Thomas, S. E. Palo, and S. M. Bailey (2003), Observations of the 5-day planetary wave in PMC measurements from the Student Nitric Oxide Explorer satellite, *Geophys. Res. Lett.*, *30*(4), 1196, doi:10.1029/2002GL016524.
- Rapp, M., and F.-J. Lübken (2004), Polar mesosphere summer echoes (PMSE): Review of observations and current understanding, *Atmos. Chem. Phys.*, *4*, 2601–2633.
- Rapp, M., and G. E. Thomas (2005^{*}), Modeling the microphysics of mesospheric ice particles—Assessment of current capabilities and basic sensitivities, *J. Atmos. Sol. Terr. Phys.*, doi:10.1016/j.jastp.2005.10.015, in press.
- Rapp, M., F.-J. Lübken, A. Müllemann, G. Thomas, and E. Jensen (2002), Small-scale temperature variations in the vicinity of NLC: Experimental and model results, *J. Geophys. Res.*, *107*(D19), 4392, doi:10.1029/2001JD001241.
- Rapp, M., F.-J. Lübken, P. Hoffmann, R. Latteck, G. Baumgarten, and T. Blix (2003), PMSE dependence on aerosol charge number density and aerosol size, *J. Geophys. Res.*, *108*(D8), 8441, doi:10.1029/2002JD002650.
- von Cossart, G., J. Fiedler, and U. von Zahn (1999), Size distributions of NLC particles as determined from 3-color observations of NLC by ground-based lidar, *Geophys. Res. Lett.*, *26*, 1513–1516.
- von Zahn, U., and U. Berger (2003), Persistent ice cloud in the midsummer upper mesosphere at high latitudes: Three-dimensional modeling and cloud interactions with ambient water vapor, *J. Geophys. Res.*, *108*(D8), 8451, doi:10.1029/2002JD002409.
- Wickwar, V., M. Taylor, J. Herron, and B. Martineau (2002), Visual and lidar observations of noctilucent clouds above Logan, Utah, at 41.7°N, *J. Geophys. Res.*, *107*(D7), 4054, doi:10.1029/2001JD001180.
- Zecha, M., J. Bremer, R. Latteck, W. Singer, and P. Hoffmann (2003), Properties of midlatitude mesosphere summer echoes after three seasons of VHF radar observations at 54°N, *J. Geophys. Res.*, *108*(D8), 9439, doi:10.1029/2002JD002442.

U. Berger and F.-J. Lübken, Leibniz Institute of Atmospheric Physics, Schloss-Strasse 6, D-18225 Kühlungsborn, Germany. (luebken@iap-kborn.de)